stance, the 31 magnitudes in its second neighborhood, have been found. Just as the analogous distributions for quartets have already proven to be useful in the applications, and the recently secured quintet distributions are sure to be useful as well, it is anticipated that the distributions derived here, in particular (3.3), will play an important role in the applications. If it should turn out that the discriminant Δ is strongly correlated with the value of the structure invariant φ, as conjectured, then the usefulness of the sextets will surely be enhanced.

It should be observed finally that in the presence of one or a few heavy atoms the distributions derived here are sharpened, thus leading to more reliable estimates of φ, as anticipated. It had been observed earlier (Hauptman, 1976; Hauptman & Fortier, 1977) that in the extreme case that $\sigma_3=0$ (possible only in the neutron diffraction case when some of the f_j may be negative) the distributions of quartets and quintets corresponding to the second neighborhood degenerated to the first-neighborhood distributions, so that nothing was gained in going to the second neighborhood. It is therefore a matter of some interest to observe that this phenomenon does not occur with sextets. Specifically, even in the extreme case that $\sigma_3=0$, the distribution (3.3) [or (3.6)] does not reduce to the distribution (4.1) so that it is still possible to use the information contained in the second neighborhood. In particular, if $\sigma_3=0$ then the dependence on the 15 cross-terms $R_{12}, \ldots, R_{56}$ is indeed lost but, as is easily verified, $\varphi \simeq 0$ or $\varphi \simeq \pi$ according as the ten cross-terms $R_{123}, \ldots, R_{156}$ are mostly large or mostly very small, respectively.

This research was supported by Grant No. MPS73-04992 from the National Science Foundation, DHEW Grant No. HL15378 and RR05716 and Ministère de l'Education, Gouvernement du Québec.

References

FORTIER, S. & HAUPTMAN, H. (1977). *Acta Cryst.* A**33**, 694–696.
HAUPTMAN, H. (1975). *Acta Cryst.* A**31**, 680–687.
HAUPTMAN, H. & FORTIER, S. (1977). *Acta Cryst.* A**33**, 575–580.

Acta Cryst. (1977). A**33**, 701–703

Structure Determination of a Mixed-Layer Bismuth Titanate, $Bi_7Ti_4NbO_{21}$, by Super-High-Resolution Electron Microscopy

BY SHIGEO HORIUCHI, TAKESHI KIKUCHI AND MASARU GOTO

National Institute for Researches in Inorganic Materials, Sakura-mura, Niihari-gun, Ibaraki, Japan 300-31

(*Received* 31 *January* 1977; *accepted* 24 *March* 1977)

The crystal structure of a bismuth titanate, $Bi_7Ti_4NbO_{21}$, was determined on the basis of super-high-resolution images, taken by a recently constructed 1000 kV electron microscope, in which each cation site was approximately defined. It was found that the crystal has a mixed-layer structure, *i.e.* $Bi_4Ti_3O_{12}$ and Bi_3TiNbO_9-like layers are alternately intergrown. The symmetry is orthorhombic with space group *I2cm*. The lattice parameters are $a=5{\cdot}45$, $b=5{\cdot}42$ and $c=58{\cdot}1$ Å. That the periodicity along **c** is twice that expected from a simple intergrowth can be accounted for by the rotation of octahedra. The lattice defects found are discussed in terms of twinning of the crystal.

Introduction

Since the work of Aurivillius (1949) it has been known that the ferroelectric bismuth titanates belonging to the $Bi_4Ti_3O_{12}$ family consist of Bi_2O_2 sheets interleaved with perovskite-like $A_{n-1}B_nO_{3n+1}$ layers, where n is an integer between 1 and 5. The cubo-octahedral A site accepts Bi, Ba, Sr, K, Ca, Na, Pb and several rare-earth ions, while the smaller Ti, Nb, Ta, Fe, W, Mo, Ga and Cr ions go into the octahedral B sites. The lattice distortions in the room-temperature phase are understood in fair detail in connexion with the ferroelectricity (Newnham, Wolfe & Dorrian, 1971).

One of the present authors (Kikuchi, 1976) recently prepared a new compound $Bi_7Ti_4NbO_{21}$ by heating mixtures of $Bi_4Ti_3O_{12}$ ($n=3$) and Bi_3TiNbO_9 ($n=2$). X-ray powder diffraction data suggested that the compound is built up by a regular intergrowth of the two starting constituents along **c**. Because of difficulty in preparing large crystals the structure analysis has not been performed.

The contrast of recent electron-microscope images roughly represents the projection of potential distributions of a crystal, when the incident beam is parallel not only to the optical axis but also to a zone axis of the crystal (Cowley & Iijima, 1972). In order to obtain good 'structure images' the resolution limit of the objective lens should be lowered so that as many scattered waves as possible contribute to forming images. An improvement of the resolution limit can be achieved by elevating the accelerating voltage unless the spherical aberration becomes too large (Scherzer, 1949). This enables us to obtain the structure images from crystals with a relatively small unit cell, which has been impossible with any 100 kV-class electron microscope.

We have recently constructed a high-voltage electron microscope (Hitachi 1250 type) designed expecially for observing high-resolution crystal structure images. It is able to resolve a lattice spacing of 2·0 Å at an accelerating voltage of 1000 kV under the condition of axial illumination with use of a goniometer stage (Horiuchi, Matsui & Bando, 1976). The measured value of the spherical aberration coefficient of the objective lens was in the range between 8 and 10 mm.

In the present paper a structure determination of $Bi_7Ti_4NbO_{21}$, which has a large unit-cell dimension in one direction, is attempted as an example of the possible applications of super-high-resolution images by the high-voltage electron microscope.

Experimental procedure

A mixture of oxides with a composition $60\,Bi_2O_3:35\,TiO_2:5\,Nb_2O_5$ was calcined at 800 °C and then melted at about 1250 °C in a 20 ml Pt crucible. It was cooled down to 950 °C at the rate of 0·5 °C min^{-1} and then left in open air. The product was an aggregate consisting of $Bi_7Ti_4NbO_{21}$ and a small amount of $Bi_4Ti_3O_{12}$ and Bi_2O_3. The crystals were washed in warm, dilute nitric acid and separated.

Lattice images were observed in the same manner as reported previously (Horiuchi & Matsui, 1974); crystals of $Bi_7Ti_4NbO_{21}$ were ground in an agate mortar and the fragments were collected on a holey carbon film. All photographs were taken at an accelerating voltage of 1000 kV. A goniometer stage of $\pm 35°$ tilt and a hair-pin type filament were used. Images from thin regions of the fragments recorded at an underfocus of 500 to 1000 Å, which were chosen from a through-focus series of images, could be interpreted intuitively. The direct magnification was $2·5 \times 10^5$ times. The astigmatism of the objective lens was corrected by observing the Fresnel fringes at the edges of the holes in the carbon supporting film.

Experimental results and interpretation

Electron diffraction patterns of various reciprocal lattice sections showed that the symmetry of the crystal is orthorhombic and that the lattice parameters are $a=5·45$, $b=5·42$ and $c=58·1$ Å, which are in a good agreement with the result from an X-ray powder diffraction study (Kikuchi, Watanabe & Uchida, 1977). Some of the diffraction patterns are represented in Fig. 1(*a*) to (*c*). Reflexions hkl with $h+k+l=$even and $h0l$ with h and $l=$even are present and therefore possible space groups of this crystal are *I2cm* or *Imcm*.

Fig. 2 is an electron-microscope image taken by the incident beam parallel to the [110] direction. The diffraction pattern from a region including that of Fig. 2 is shown in Fig. 1(*a*), in which the position of the objective aperture used was indicated. Its size corresponds to about 0·5 $Å^{-1}$ in reciprocal space. About 80 scattered waves were used in forming images. The image contrast consists of two types of bands with different widths that appear alternately and are separated by dark zigzag lines.

Fig. 3(*a*) is an enlargement of a portion of Fig. 2. The contrast can well be accounted for on the basis of the known structures of $Bi_4Ti_3O_{12}$ and Bi_3TiNbO_9. The former has a three-layer structure and corresponds to the wide band in the figure. The latter with a two-layer structure corresponds to the narrow band. The regions with dark zigzag contrast may correspond to Bi_2O_2 sheets. Fig. 3(*c*) shows an idealized structure model. The correspondence between the contrast and the atom positions is shown in Fig. 3(*b*). It is obvious that the sites of cations show dark contrast, while those of O atoms are bright. The contrast of a cation site links to that of an adjoining site to form a dark line.

Fig. 4(*a*) is an image taken from another crystal but with the incident beam parallel to the [100] direction. The corresponding diffraction pattern is shown in Fig. 1(*b*). The image contrast can also be interpreted on the basis of the intergrowth of $Bi_4Ti_3O_{12}$ and Bi_3TiNbO_9-like layers along **c**. It is likewise noted that regions with cation sites show dark contrast, with reference to Fig. 4(*b*) & (*c*). O atoms do not necessarily correspond to the sites of white contrast in this case.

The image taken with the incident beam parallel to the [010] direction is similar to that of Fig. 4(*a*). The corresponding diffraction pattern is shown in Fig. 1(*c*).

It is concluded from these observations that the positions of cations are almost the same as those in $Bi_4Ti_3O_{12}$ and Bi_3TiNbO_9 compounds. It may be considered that the crystal symmetry of $Bi_7Ti_4NbO_{21}$ is determined by the arrangements of O atoms, in other words, by the manner of octahedral rotation, as was the case for the latter two compounds.

Taking account of these conditions we tried to construct a structural model; one of the space groups mentioned above, *Imcm*, is unlikely since the octahedral cations responsible for the ferroelectricity are considered to be shifted in one direction along **a**. Finally, we choose the model shown in Fig. 5; octahedra are slightly rotated about **a** because of the strong bondings of the apex O atom with Bi ions in the Bi_2O_2 sheet. The rotational direction is reversed in every second layer. The periodicity along **c** is twice that expected from a pair of narrow and wide bands. The rotations of octahedra about **c** and the displacements of octahedral cations are the same as those in $Bi_4Ti_3O_{12}$ or Bi_3TiNbO_9.

Lattice defects are found at the regions marked by

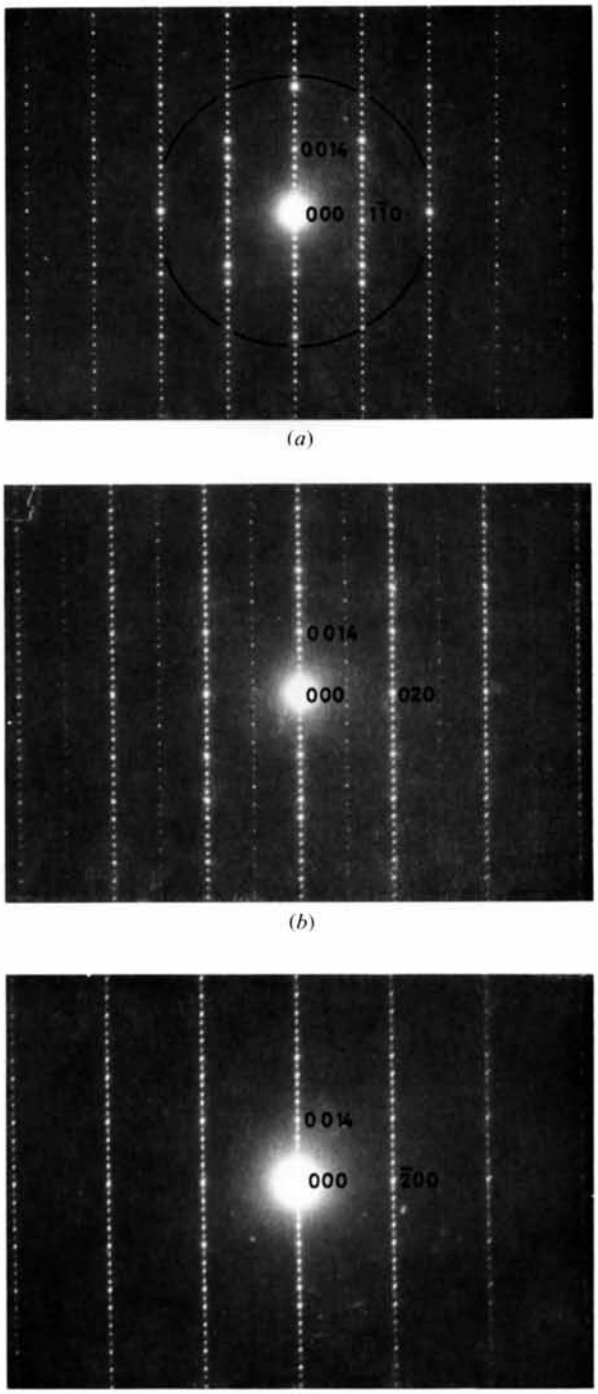

(a)

(b)

(c)

Fig. 1. Electron diffraction patterns of $Bi_7Ti_4NbO_{21}$. The electron beam is incident parallel to (*a*) [110], (*b*) [100] and (*c*) [010].

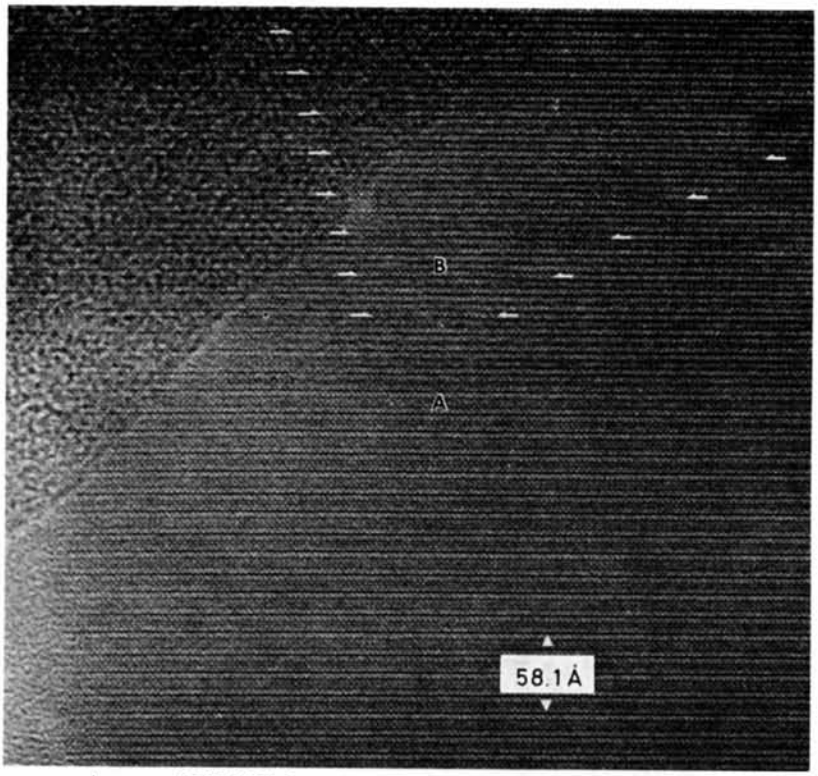

Fig. 2. An electron microscope image of $Bi_7Ti_4NbO_{21}$ taken at 1000 kV. The crystal is oriented so that the [110] zone axis is parallel to the incident electron beam. The selected-area diffraction pattern is shown in Fig. 1 (*a*). At the portions marked by arrows lattice defects are noticed. The upper left is covered by a carbon film supporting the crystal.

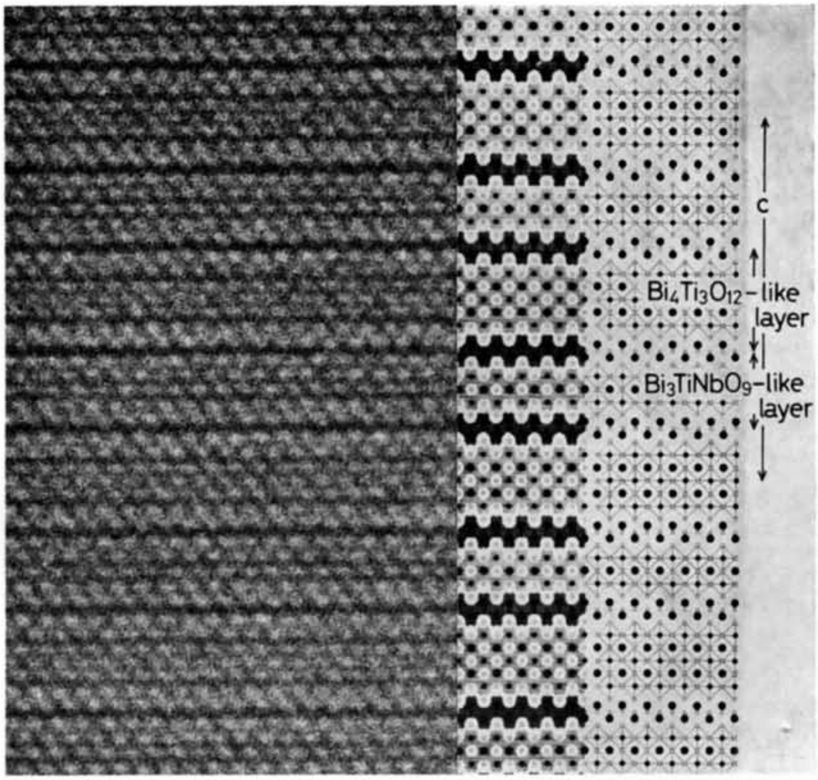

(*a*) (*b*) (*c*)

Fig. 3. Interpretation of the image contrast in Fig. 2. (*a*) An enlarged image of a portion of Fig. 2. (*b*) The correspondence between the image contrast and the crystal structure. (*c*) The prototype structure of $Bi_7Ti_4NbO_{21}$ viewed along [110]. Large dark circles indicate Bi ions., small circles Ti or Nb ions and open circles O ions. $c = 58.1$ Å.

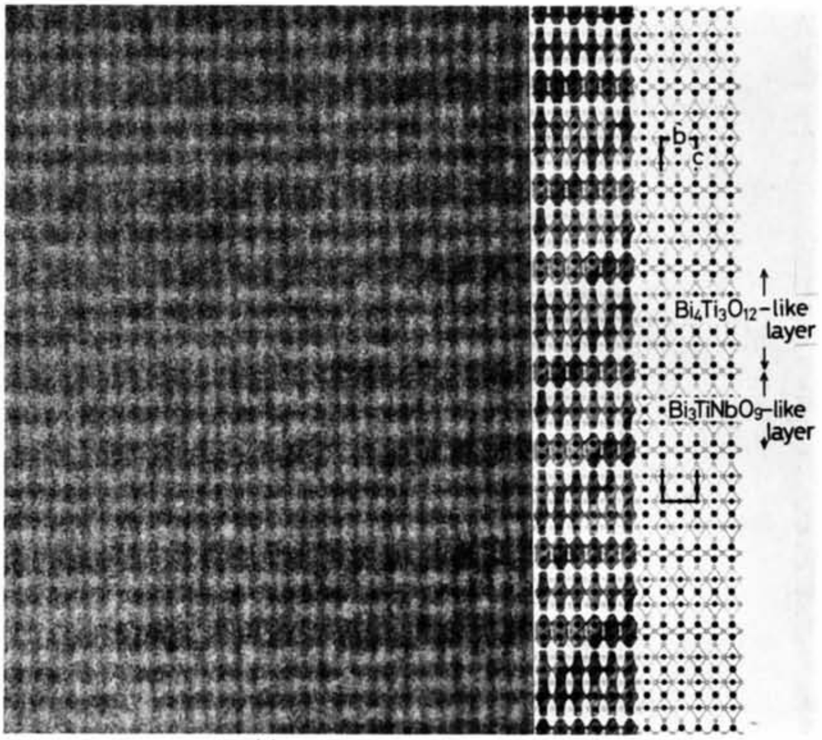

(*a*) (*b*) (*c*)

Fig. 4. A structure image of $Bi_7Ti_4NbO_{21}$ with (*a*) the [100] zone-axis orientation. The corresponding diffraction pattern is shown in Fig. 1 (*b*). (*b*) The correspondence between the image contrast and the crystal structure. (*c*) The prototype structure. Large dark circles indicate Bi ions, small circles Ti or Nb ions and open circles O ions. Octahedra centred at $x = a/2$ are shown by dotted lines, those at $x = 0$ by solid lines. The unit cell is outlined; $b = 5.42$ and $c = 58.1$ Å

arrows in Fig. 2. Atomic displacements causing these defects are schematically shown in Fig. 6. A Bi_2O_2 sheet displaces parallel to **c** direction by a distance of one octahedron so that the narrow and wide bands are mutually substituted. A similar defect structure was observed near the dislocation core in $Ba_2Bi_4Ti_5O_{18}$ by a 100 kV-electron-microscope lattice image (Hutchison, Anderson & Rao, 1975). In the present case the defects occur in every second Bi_2O_2 sheet. A periodic occurrence of defects is discussed below in terms of twinning.

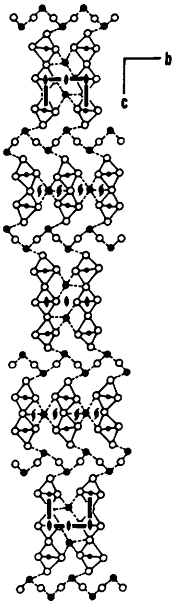

Fig. 5. A structure model proposed for $Bi_7Ti_4NbO_{21}$ viewed along [100]. The symbols have the same meanings as those in Fig. 3. Octahedra centred at $x=a/2$ are abbreviated for simplicity. The unit cell is outlined. The symmetry is orthorhombic with space group *I2cm*. The lattice parameters are $a=5{\cdot}45$, $b=5{\cdot}42$ and $c=58{\cdot}1$ Å.

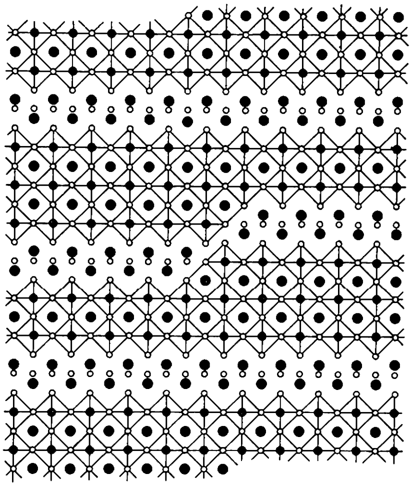

Fig. 6. A schematic representation of the defect structure observed in Fig. 2. The symbols have the same meanings as those in Fig. 3.

Discussion

The stacking of the layers along **c** of $Bi_7Ti_4NbO_{21}$ can be described as $\ldots WNW'N'WNW'N'\ldots$, where W denotes the wide $Bi_4Ti_3O_{12}$-like layer and N the narrow Bi_3TiNbO_9-like layer. The prime is to distinguish the rotational direction of octahedra in each layer. Once narrow layers adjoin at the region of the defects as seen in Fig. 2, the stacking of layers along the line A–B is considered to be $\ldots WNW'N'N'W'NW\ldots$. The crystal orientations in the two areas divided by the array of the defects are therefore twin-related with respect to one another.

The fact that the c lattice parameter is twice that expected from a simple intergrowth is substantially due to the Bi_3TiNbO_9-layer having the two-layer structure with a mirror symmetry perpendicular to **c**, while the $Bi_4Ti_3O_{12}$-like layer has the three-layer structure with two-fold symmetry. The similar periodicity along **c** is expected to exist in all mixed-layer bismuth titanates since they are composed of a pair of even and odd-layer components. This has been confirmed in a compound, $SrBi_8Ti_7O_{27}$,* which gave electron diffraction spots with the same excitation rule as $Bi_7Ti_4NbO_{21}$ and had the c parameter equal to the sum of those of the component compounds, $Bi_4Ti_3O_{12}$ and $SrBi_4Ti_4O_{15}$.

The authors wish to express their deep gratitude to Dr I. Kawada for valuable discussion.

References

Aurivillius, B. (1949). *Ark. Kem.* **1**, 463.

Cowley, J. M. & Iijima, S. (1972). *Z. Naturforsch.* **27a**, 445–451.

Horiuchi, S. & Matsui, Y. (1974). *Phil. Mag.* **30**, 777–787.

Horiuchi, S., Matsui, Y. & Bando, Y. (1976). *Jap. J. Appl. Phys.* **15**, 2483–2484.

Hutchison, J. L., Anderson, J. S. & Rao, C. N. R. (1975). *Nature, Lond.* **225**, 541–542.

Kikuchi, T. (1976). *J. Less-Commom Met.* **48**, 319–323.

Kikuchi, T. (1977). *J. Less-Commom Met.* **52**, 169–171.

Kikuchi, T., Watanabe, A. & Uchida, K. (1977). To be published.

Newnham, R. E., Wolfe, R. W. & Dorrian, J. F. (1971). *Mater. Res. Bull.* **6**, 1029–1040.

Scherzer, O. (1949). *J. Appl. Phys.* **20**, 20–29.

---

* A description of the synthesis of this compound has been reported elsewhere (Kikuchi, 1977).